



VULNERABILITY OF RC FRAME STRUCTURES IN TURKISH EARTHQUAKE REGIONS (PART 2): MODELING AND ANALYSIS

Lars ABRAHAMCZYK¹, Corina SCHOTT², Jochen SCHWARZ³ and Thomas M. SWAIN⁴

SUMMARY

The aim of these investigations is to estimate the vulnerability of typical building types found in earthquake-prone regions, of which Turkey is a prominent example. Detail is added to the analyses by considering those subsoil conditions laid out in part 1 of the paper (Lang et al. [8]), the use of two different software engineering applications (ETABS Nonlinear and SLang [2]) and the calibration of models regarding stiffness behavior. A suggestion is made for how to clearly specify damage grades, in order that effective analysis during damage surveys can be performed.

In the first step, nine representative buildings from the Turkey were selected and all data pertaining thereto collected. The buildings were surveyed in states of construction either as pure RC building shells or as RC shells with brick walls filled in the spaces. The results of dynamic tests on the structures and subsoil are described in Part I and used later to calibrate virtual models and determine soil characteristics.

After the structural parameters are determined, the capacity or “pushover” curves for the individual buildings are calculated, including corresponding damage patterns for increasing load levels.

Subsequently, by applying the capacity spectrum method, the performance point of the building at the given input seismic action is determined, which is derived from records of the 1999 Kocaeli earthquake at or near the respective site (see part 1 of the paper). By this procedure a specific damage state corresponding to the given seismic action results, which is then compared to the damage that actually occurred. Further calculations are carried out in order to estimate the building’s reaction to the required design spectrum and to determine the ultimate load capacity by scaling the design spectrum and the recorded time history.

¹ Research assistant, Earthquake Damage Analysis Center (EDAC), Bauhaus-University Weimar, Germany. Email: lars.abrahamczyk@bauing.uni-weimar.de

² Research assistant, Earthquake Damage Analysis Center, Bauhaus-University Weimar, Germany.

³ Head of Earthquake Damage Analysis Center, Bauhaus-University Weimar, Germany.

⁴ Research assistant, Earthquake Damage Analysis Center, Bauhaus-University Weimar, Germany.

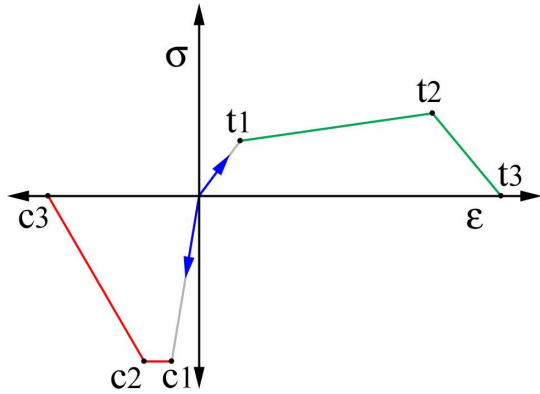


Figure 1. Nonlinear stress-strain behavior with distinct compression and tension parameters added to SLang by Swain.

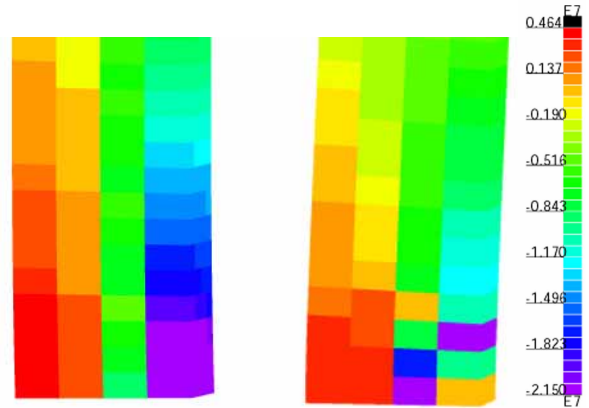


Figure 2. Damage state of columns can be derived from stress distribution: left column not damaged, right column damaged (SLang [2]).

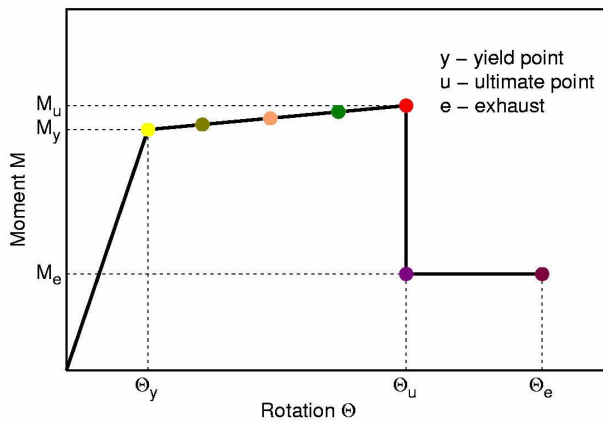


Figure 3. Moment-rotation relationship for RC elements (ETABS).

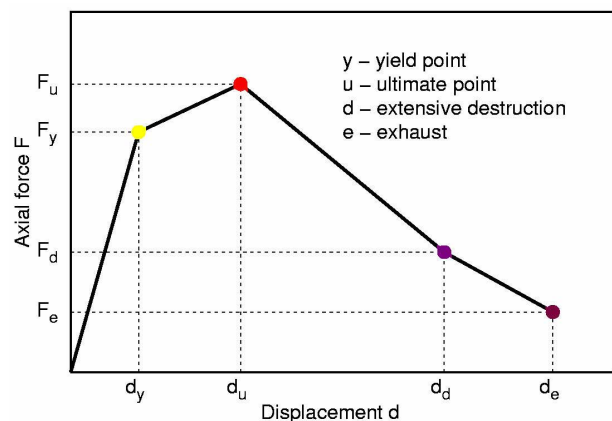


Figure 4. Force-displacement relationship for diagonal struts for masonry infills (ETABS).

APPLIED SOFTWARE TOOLS

SLang - The Structural Language

SLang is a program system developed for mechanical and structural engineers at the Bauhaus-University Weimar [2]. It is capable of combining static or dynamic finite element calculations with stochastic, probabilistic, and optimization procedures. In this case the capacity curves (base shear versus top displacement) of the investigated objects were calculated; thus static non-linear analysis was used.

The finite element type currently available for the analysis of RC frame buildings is a beam element with a 4 x 4 grid of integration points in the section. In order to simulate the behavior of RC, a nonlinear material law was implemented by Swain, which allows the assignment of distinct material parameters for the tension and compression domain (cf. Figure 1). Here the material parameters for compression were derived from concrete stress-strain diagrams, and the material parameters for tension were taken from the stress-strain behavior of the reinforcing steel, taking the reinforcement ratio into account.

The use of finite elements for modeling RC structures under seismic loads has particular strengths in the accurateness of three-dimensional interaction of forces and in simplicity of use. In the initial stage, the

geometry of the RC elements is modeled in greater detail by using, for instance, beam elements with a grid of integration points, to which the nonlinear behavior of the concrete and the longitudinal reinforcement is assigned. To do this, information about the stress-strain behavior of the materials must be available. Once this procedure has been conducted, the nonlinear deformation of the structure can be calculated without any need of further specifications, as the ductility of the RC elements results from the sum of the stress-strain behavior of the individual integration points. Different situations of normal force or element geometry are automatically taken into account.

Nonlinear reactions during a “pushover” or time history calculation can be identified by a sudden change in stress distributions in the critical elements. On the left side of Figure 2, a typical stress distribution is shown in a column with high load, with the ultimate tensile stress reached in the tension zone (red) and the ultimate compressive stress reached in the compression zone (violet). If the horizontal load is raised further, failure of the compression zone occurs, with stresses falling sharply to low stress regions or zero (orange). The stress distribution in the column on the right side of Figure 2 shows this effect. This column, though not yet collapsed, has lost the greater part of its resistance against moment load.

ETABS Nonlinear

The classical approach, which is used by ETABS, is to consider single elements as ideal beams with corresponding yield moments, which are calculated by taking sectional parameters, including reinforcement, into account. Nonlinear reactions are considered by modeling nonlinear links with plasticity concentrated in points at the ends of each element. The deformation capacity of the elements is derived by firstly determining the rotation corresponding to the yield moment. The rotation corresponding to the failure point is subsequently calculated by applying the previously defined rotational ductility, resulting in a moment-rotation-relationship as shown in Figure 3. However, a problem arises when using this method, as the yield moment, the yield rotation and the ductility vary depending on the normal force. Normal forces mostly do not change much during a static nonlinear analysis with seismic load. An important advantage of the classical approach is the existing wide-spread experience with it.

For the modeling of walls fitted into RC frames, diagonal struts with nonlinear behavior as illustrated in Figure 4 are available (Further details given in section *Modeling of Buildings*).

ASSIGNMENT OF DAMAGE GRADES

Why use damage grades?

Observed damages and recorded data, be they from actual earthquakes or experiments, are essential for the calibration of software tools for seismic analysis. One important aim of this procedure is to improve the accuracy of damage state calculations for specific buildings at a given specific seismic load. This is not the only use of such procedures, though. A further goal is to establish or improve methods of loss estimation for entire building stocks at varying levels of seismic action. Information about this is needed by public authorities, emergency aid organizations and insurance companies. The introduction of damage grades at this point is motivated by the necessity to compare calculated results with observed building reactions on a greater scale.

Current situation

Damage grades are roughly defined in EMS-98 [7]. The current definition applicable to RC buildings is given in the first column of Table 1. A more detailed definition, however, which could be applied directly and unambiguously both by scientists involved in damage calculations and by practical engineers or operators surveying damaged building stock, has yet to be agreed upon.



Figure 5. RC building shell Sultandağı (SUL).

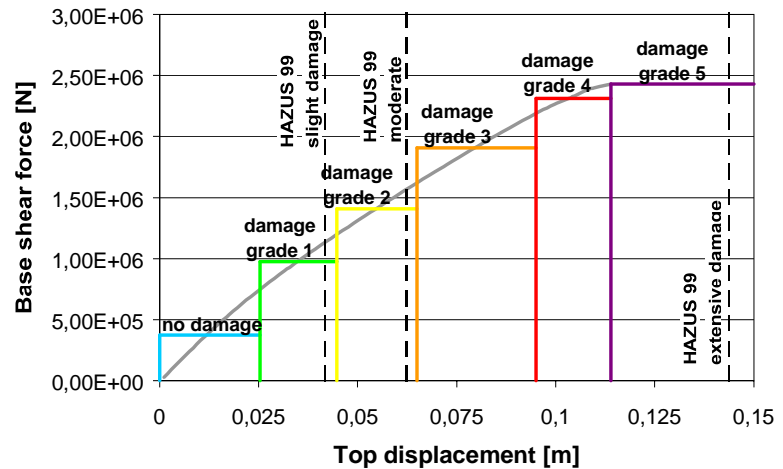


Figure 6. Capacity curve of RC building SUL with assigned damage grades; comparison to damage according to building type C1M pre-code in HAZUS 99 [6].

The following is stated in EMS-98, Section 1.2.2: “Grades 1 to 5 should ideally represent a linear increase in the strength of shaking ... They do this only approximately, and are heavily influenced by the need to describe classes of damage which can be readily distinguished by the operator.” The first provision is then put into perspective by referring to the case of buildings with earthquake resistant designs, which are expected to react highly nonlinear and should reach a saturation of damage at grades 2 and 3, which remain valid for a wide range of seismic shaking intensity.

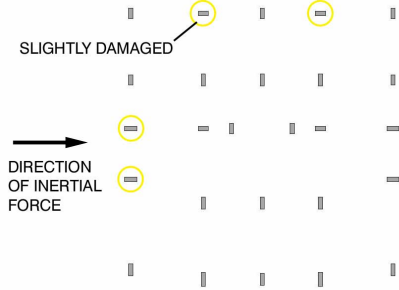
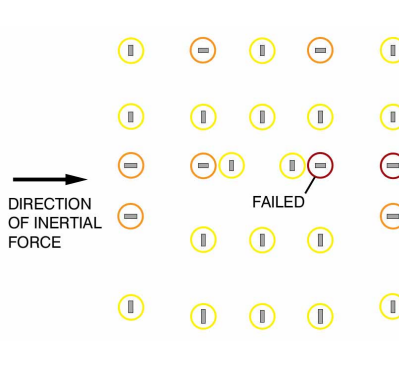
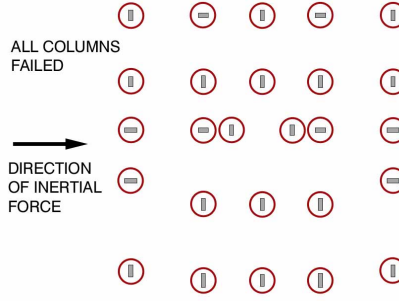
A possible variation on the first provision is to say that the damage grades should ideally represent a linear decrease in the energy dissipation reserves remaining in the structure (using integration of the force-displacement-curve as a measure for the dissipated energy). This would yield a more accurate evaluation of the remaining earthquake resistance of highly engineered structures.

However, while this approach would make sense for the mechanical engineer, there are other aspects which might have differing priorities. For instance, insurance companies would supposedly prefer a damage classification to reflect the level of financial loss. Furthermore, a very important issue is raised in the second provision above: To be practicable, the damage grades must be readily distinguishable by the operator, the person surveying the damage. In damage surveys after an earthquake, large amounts of buildings generally have to be classified in a short amount of time. Therefore, the openly visible, or in a simple way discernible, damage must be used as the main criterion.

Proposed approach for more detailed definition of damage grades by Swain and Schwarz [10]

As already pointed out, a rough description of the damage states associated with the damage grades is given in EMS-98. While the main phenomena regarding structural and nonstructural damage are described, there is no detailed statement regarding the extent or quantification of the given main phenomena. A possible approach would be to simply count the number of affected elements (be it columns or walls reaching from one floor to the next, or beams spanning from one column to the next) with a certain damage state. The amount of affected elements could then be related to a certain reference group of relevant elements, as proposed by Swain and Schwarz [10]. To simply relate the number of affected elements to the total number of elements of the entire building would be a weak indicator.

Table 1. Classification of damage to RC buildings, including proposed refinements and examples.

Damage grade definition according to EMS-98 [7]	Proposed refinement to definition	Corresponding damage state of example building SUL
<p>DG 1: Negligible to slight damage (no structural damage, slight non-structural damage) Fine cracks in plaster over frame members or in walls at the base. Fine cracks in partitions and infills.</p>	<p>No further differentiation proposed</p>	<p>No structural damage</p>
<p>DG 2: Moderate damage (slight structural damage, moderate nonstructural damage) Cracks in columns and beams of frames and in structural walls. Cracks in partition and infill walls, falling of brittle cladding and plaster. Falling mortar from the joints of wall panels.</p>	<p>Most elements of the relevant element group show cracks (the group of elements relevant for a typical seismic load pattern must first be identified, either by calculation or experience).</p>	
<p>DG 3: Substantial to heavy damage (moderate structural damage, heavy nonstructural damage) Cracks in columns and beam column joints at the base and at the joints of coupled walls. Spalling of concrete cover, buckling of reinforced rods. Large cracks in partition and infill walls, failure of individual infill panels.</p>	<p>Most elements of the relevant element group show large cracks and/or spalling of concrete cover and buckling of reinforcement (the group of elements relevant for a typical seismic load pattern must first be identified, either by calculation or experience).</p>	
<p>DG 4: Very heavy damage (heavy structural damage, very heavy nonstructural damage) Large cracks in structural elements with compression failure of concrete and fracture of rebars, bond failure of beam reinforced bars, tilting of columns. Collapse of a few columns or of a single upper floor.</p>	<p>Many (more than 25 %, for example) elements of the relevant element group show compression failure of concrete and/or fracture of reinforcement bars (the group of elements relevant for a typical seismic load pattern must first be identified, either by calculation or experience). Collapse of small part of total ground area smaller (e. g. 10 %) tolerated.</p>	
<p>DG 5: Destruction (Very heavy structural damage) Collapse of ground floor or parts (e. g. wings) of buildings.</p>	<p>Collapse of more than small part of (e. g. 10 %) total ground area.</p>	

A group of relevant elements can only be defined with some knowledge about the failure mechanism. Given a specific load pattern, it is generally possible to detect certain elements which attract more forces in relation to their capacity than the others. In most cases, these elements would also be mainly responsible for the structure's resistance to the specific load, and failure of these elements would lead to the failure of the structure. It therefore suffices to observe the performance of this particular group of elements to gain an idea about the safety of the whole building.

The load pattern to be expected during seismic action on a building is known approximately, with the main uncertainty being the incoming direction of the shock waves in the horizontal plane.

In the second column of Table 1 proposals for a clearer and more detailed definition of damage grades 2 to 5 are presented based on the performance of a relevant element group.

Example

In the course of nonlinear analysis, the investigated Turkish RC frame buildings of multiple stories were subjected to pushover analysis. For example, Figure 6 shows the resulting capacity curve of the RC building shell SUL (photo in Figure 5) for seismic load in the x-direction. The curve is split into portions assigned to increasing damage grades, including a comparison to damage states acc. to HAZUS 99 [6].

The results of the calculation indicate that the critical elements are almost always the ground floor columns, which corresponds well with observed damages. However, a different selection of ground floor columns is affected depending on the direction of incoming forces.

The columns of the investigated structures typically had wall-like dimensions with a long side (60 – 175 cm) and a short side (20 – 25 cm). Consequently, the stiffness and load bearing resistance of the individual column differed considerably depending on the direction of horizontal load. Thus, for a force in the x-direction, columns with their long sides parallel to the x-axis (*x-oriented*) were first activated and responsible for the major part of the load bearing capacity of the whole structure. This effect is also visible in the reaction of the RC building SUL to inertial forces in x-direction. For this example, then, ground floor columns oriented in the x-direction were selected as the reference element group.

Having identified the relevant elements for the failure mechanism, the procedure of assigning a damage grade can now be carried out by surveying the extent of damage on this particular group. Theoretically, these elements should be the most heavily affected elements of the structure. The description of the damage characteristics for each damage grade can now be taken from EMS-98 and applied to the relevant element group. The right side of Table 1 shows the calculated damage states of the ground floor columns, which were assigned to damage grades 2 to 5.

Problem: uncertainty of direction of incoming forces

On the other hand, for the example building SUL, a horizontal force in the y-direction would mainly activate columns with a y-orientation, and after these failed, the remaining columns would not be able to offer significant resistance any more. Thus the analysis of the two main directions yields two different groups of relevant elements. These should be evaluated separately, and the more severe classification should be regarded as valid for that particular building.

After an earthquake, the exact direction of incoming forces is rarely known, unless recorded data is at hand. It is also uncertain whether the next shock will come from the same direction. It is therefore sensible to check the damage state for any incoming direction and choose the highest resulting damage grade.

Given a regular symmetrical column grid, either of the two main directions (transversal and longitudinal building axes) generally bears the least resistance to horizontal forces. For irregular structures, incoming horizontal forces at varying angles should be considered as well.

MODELING OF THE BUILDINGS

Basics

A detailed description of the modeling procedure and subsequent calculations is given by Schott et al. [9]. For the buildings investigated, three-dimensional models were created using the software tools ETABS and SLang. Construction plans and on-site surveys of the buildings supplied the required geometrical data. In some cases, the geometry of the buildings as surveyed on site deviated from the construction plans. Such deviations were noted and included in the models.



Figure 7. RC building shell İzmit-2a (IZT-2a).

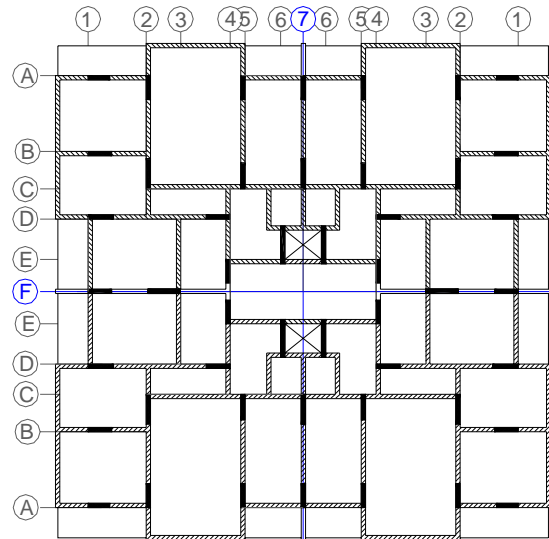


Figure 8. Layout of ground floor (IZT-2a).



Figure 9. RC frame building shell with masonry infill walls Düzce-1 (DUZ-1).

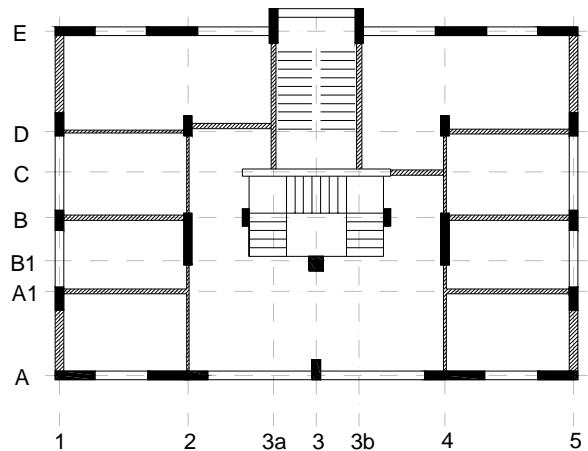


Figure 10. Layout of ground floor (DUZ-1).

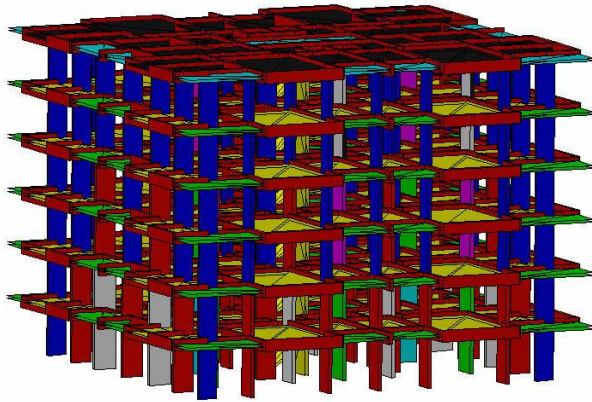


Figure 11. SLang-model of RC building shell (IZT-2a).

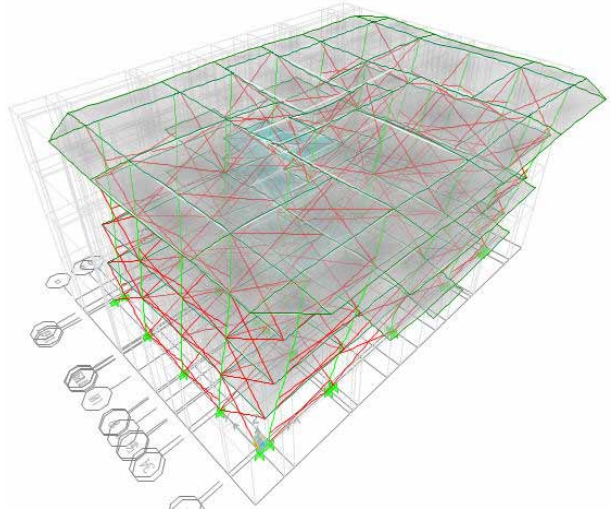


Figure 12. ETABS-model of RC building shell with masonry infill walls (DUZ-1).



Figure 13. Northern view of DUZ-1.

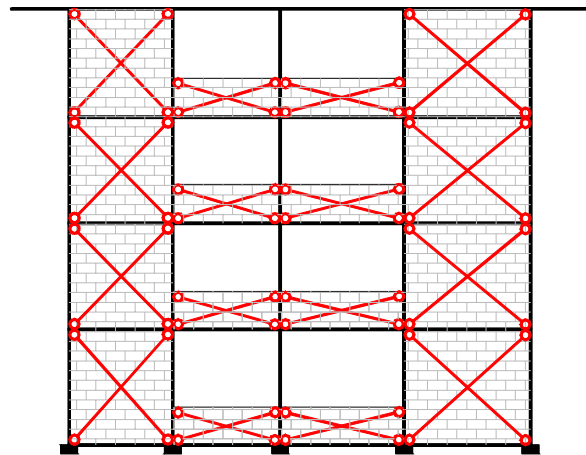


Figure 14. ETABS-model of RC frame with diagonal struts (DUZ-1).

Columns were generally assumed as rigidly connected to the underground. For buildings with a subterranean level, the support points of the column were assumed to be at medium depth of the underground story. Floors were modeled as rigid diaphragms; roof constructions were taken into account by planar loads.

The procedure of the calculations will be illustrated below on two structures. The building İzmit-2a (cf. Figures 7, 8, 11) serves as an example of a pure RC building shell, which had no infills at the time of investigation. The analysis procedure for a building with masonry infill walls is shown using building Düzce-1 (cf. Figures 9, 10, 12, 13, 14) as an example.

RC material

The material parameters for concrete were assumed to have a characteristic cube strength of 25 MPa (as denoted in construction plans and confirmed by strength tests on site using the Schmidt-Hammer).

Reinforcement was assumed to be of Turkish steel grade S420a (420 MPa yield strength, 500 MPa ultimate strength and 10 % strain at ultimate strength; generally smooth, not profiled), also corresponding with specifications in plans.

Masonry infills

Either linear elastic shell elements (SLang) or diagonal struts (ETABS, cf. Figure 14) were used for modeling the masonry infill walls. The method using diagonal struts is described in FEMA 306 [5]. In some cases the stiffness of the walls was regarded as negligible, and merely their masses were considered. The material parameters assumed for the brickwork correspond to the values of vertically perforated bricks of strength class 8 and mortar group I according to the German code for masonry structures DIN 1053-1. For nonlinear calculations the parameters defining the force-displacement relationship of the masonry infills (cf. also Figure 4) were determined according to Fajfar et al. [4].

CALIBRATION OF STIFFNESS PARAMETERS

Procedure

The fundamental periods of the buildings, which were known due to the dynamic recordings (see part 1 of the paper: Lang et al. [8]), were used as a measure for the calibration of the stiffness parameters. Young's Moduli were reduced (in comparison to recommended values given in code specifications) for all elements of identical material. The goal was not to achieve a perfect match for the individual building, but to derive a transferable reduction factor or at least tendency, which could then be applied to other buildings of the same type.

Congruency of the main mode shapes and frequencies/periods was nevertheless seen as important. A good agreement of fundamental frequencies after calibration could partly be achieved only for the first mode shape. Deviations of the second fundamental frequency did occur.

Results of calibration

Most of the nine calibrated buildings showed a strong reduction of stiffness reduction of approx. 50 %, which would correspond well to recommendations given in EC 8 for cracked RC. It appears that this stiffness can be attributed to a state of slight damage due to a former earthquake. With one exception, structures with no visible damage showed no reduction in stiffness.

The resulting stiffness reduction factors the investigated structures are as follows:

- *Slightly damaged RC frame systems without infills* 0.4 to 0.5
- *Slightly damaged RC frame system with infills* approx. 0.5
- *Undamaged RC frames with infills* twice 1.0 once 0.5

OBSERVED PAST PERFORMANCE AND ESTIMATED FUTURE EARTHQUAKE RESISTANCE

Capacity Curves İzmit-2a (IZT-2a)

As can be derived from Figure 17, the pushover calculations with ETABS and SLang resulted in capacity curves nearly identical in the linear range and the ultimate top displacement. The remaining differences, especially in the ultimate base shear force, may be explained by differences in the approach. Through the use of finite elements with spread plasticity, higher reserves in load bearing capacity are activated than in the ETABS model with lumped plasticity and abrupt loss of stiffness. The capacity curves were used to calculate the performance of the building regarding both time history and design spectrum excitation. A more detailed description of the calculations is found in [9].

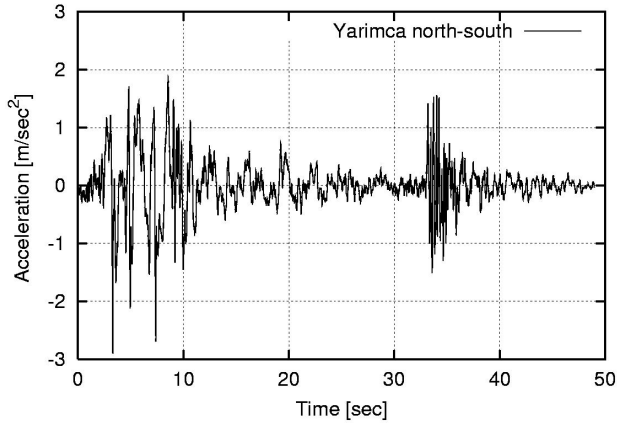


Figure 15. Time history of Yarimca, component NS.

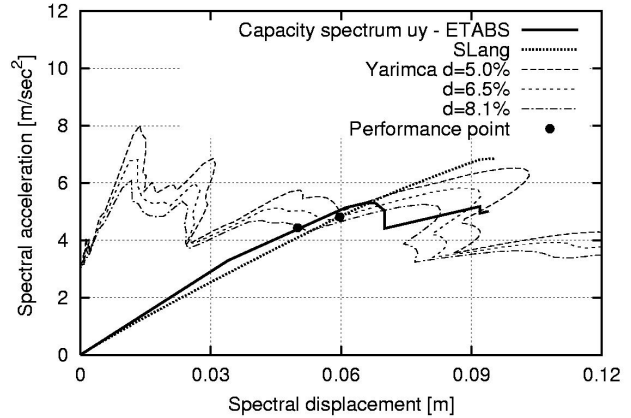


Figure 16. Results of capacity spectrum method on İzmit-2a model.

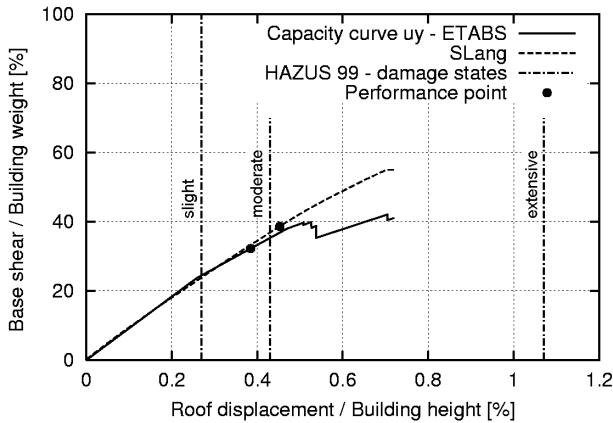


Figure 17. Capacity curves in transverse direction (IZT-2a).

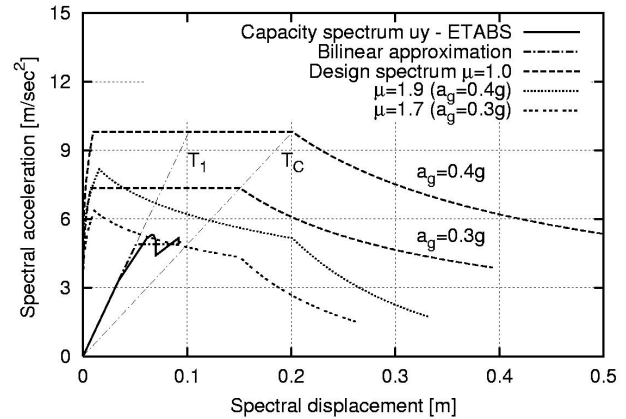


Figure 18. Application of N2-method (IZT-2a).

İzmit-2a time history excitation

The recording of the station Yarimca (Figure 15) was used as seismic excitation. During the main shock of the Kocaeli earthquake in August 1999, $PGA = 0.29g$ and $PGA = 0.24g$ were observed at this station in north-south and east-west directions, respectively. The capacity spectrum method laid out in ATC-40 [1] was applied to the structure in order to determine the performance point. According to this procedure, the intersection of the structure's capacity spectrum and the demand spectrum of the time history yields the performance point of the structure.

The derivation of the performance points of İzmit-2a for the capacity curves of ETABS and SLang are shown in Figure 16. The results are also marked in Figure 17 with the capacity curves in original format, which shows that the ETABS result lies in the range of "slight" damage according to definitions in HAZUS 99, whereas the SLang result touches on the more severe, in this case "moderate", damage state. The calculation indicates slight damage in some ground floor columns and yielding in beams (cf. Figure 19), a result which is confirmed by the survey of the damage in the original building (Figures 21, 22).

Calculations in both ETABS and SLang revealed the ground floor columns as the critical elements and the first to fail in an earthquake event. Figure 20 shows the stress situation in the ground floor columns at the ultimate load according to the SLang calculation (viewed from below).

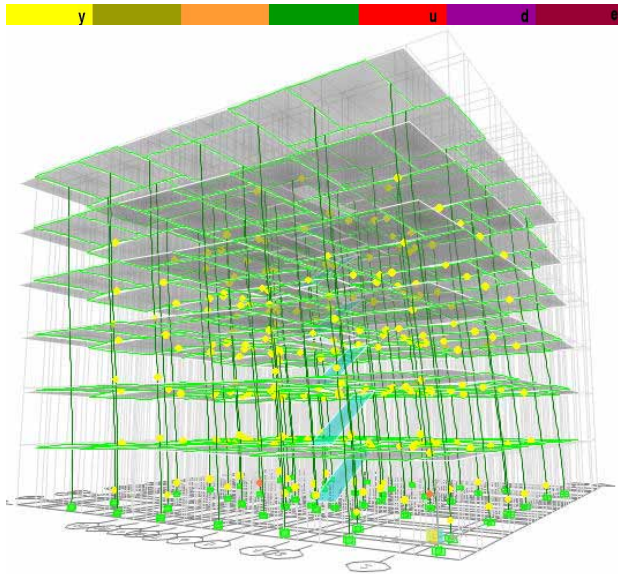


Figure 19. Damage state (IZT-2a) at performance point calculated with ETABS.

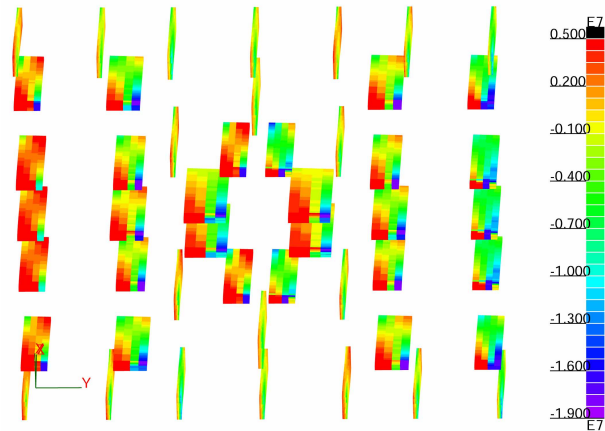


Figure 20. Stresses in ground floor columns (IZT-2a) at ultimate force calc. with SLang.



Figure 21. Observed damage at ground floor level (IZT-2a).



Figure 22. Observed damage in connection point at ground floor level (IZT-2a).

İzmit-2a design spectrum excitation

Another interesting result is shown in Figure 18. The N2-method proposed by Fajfar [3] was applied to investigate the response of IZT-2a to a design spectrum excitation. A design spectrum according to the Turkish seismic code and assuming seismic zone Z4 (PGA=0.4g), factor of building importance class I=1.0, and soft subsoil conditions was used. No intersection between the capacity spectrum and the design spectrum resulted; thus, according to the calculations performed here, the building would not be able to withstand an earthquake corresponding to the required specifications. Further calculations were carried out in order to determine the level of peak ground acceleration the building could resist. The value of PGA=0.3g was found to be the threshold for total collapse.

Capacity curves and damage progression of Düzce-1 (DUZ-1)

Pushover analysis (Figures 23 and 24) on the building Düzce-1 (for details see Schott et al. [9]) were analyzed exclusively using ETABS, since wall elements with the required nonlinear behavior are not yet available in SLang. The results indicate that brickwork of low strength was used for the infills. For this

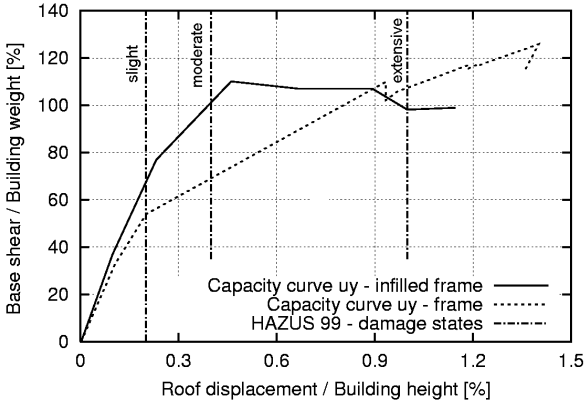


Figure 23. Capacity curve in transverse direction of DUZ-1, calculated with ETABS.

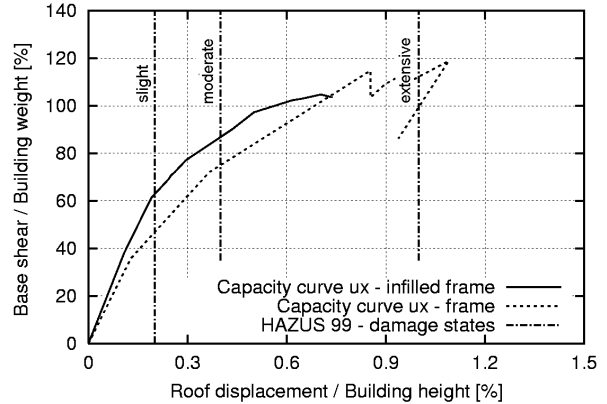


Figure 24. Capacity curve in longitudinal direction of DUZ-1, calculated with ETABS.

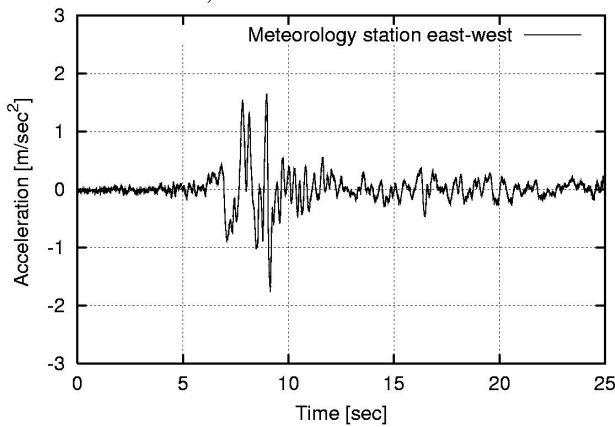


Figure 25. Time history meteorology station, component EW.

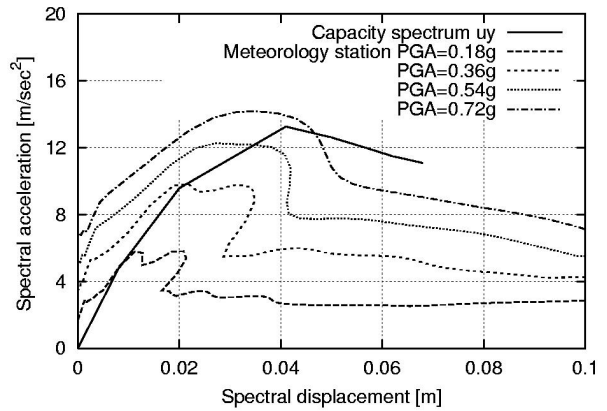


Figure 26. Results of capacity spectrum method on DUZ-1 model.

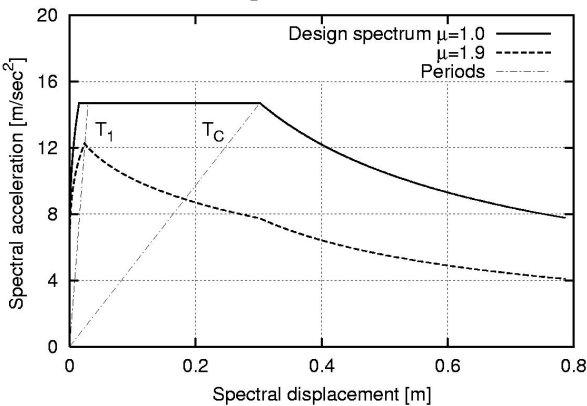


Figure 27. Demand spectrum (DUZ-1).

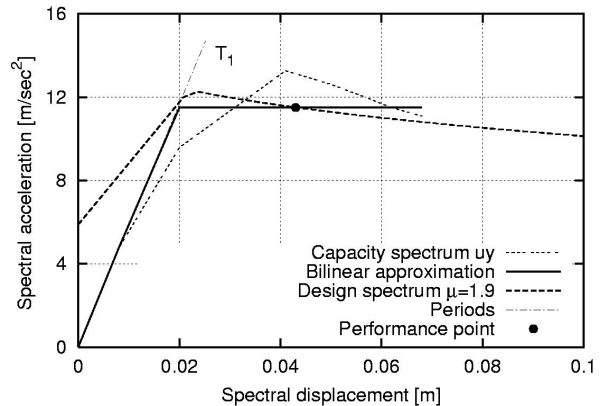
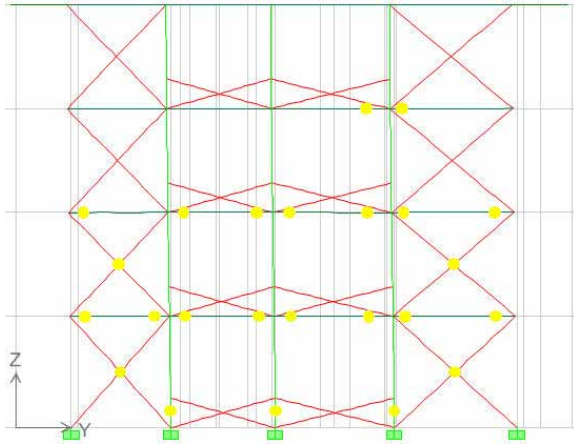


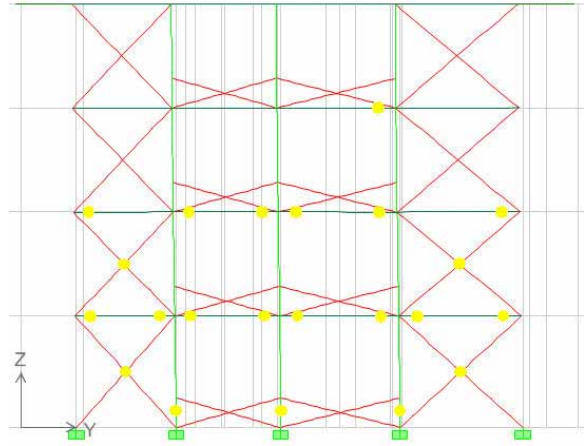
Figure 28. Application of N2-method (DUZ-1)

reason, the ultimate resistance of both models (infilled and bare frame) is nearly the same. The masonry infills, however, do have an impact on the stiffness, causing it to increase. The HAZUS 99 [6] damage states displayed in Figures 23, 24 are shown for RC frames with masonry infills (Type C1M pre-code).

An interesting effect occurs in the development of the capacity curve: Both the south and north façade frames display an almost identical damage pattern at the threshold of HAZUS 99 slight damage state, as can be derived from Figure 29 (a) and (b). At this load level some of the infills are slightly damaged, but

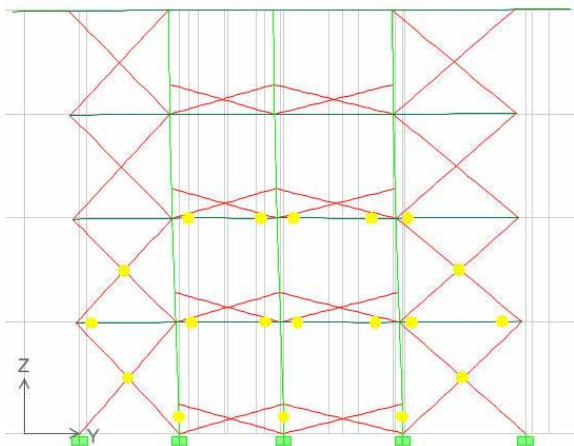


(a) South facade

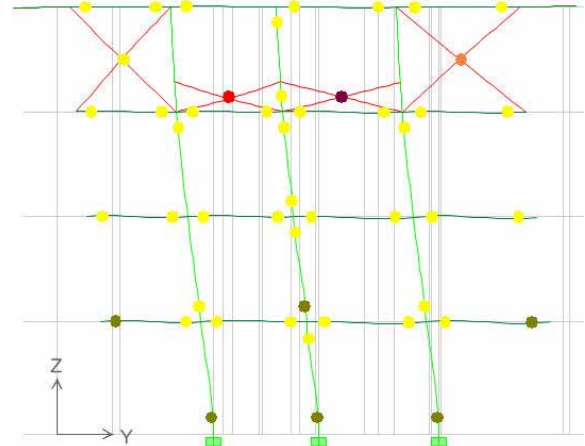


(b) North facade

Figure 29. Calculated damage progression (ETABS) at slight damage state (HAZUS 99).

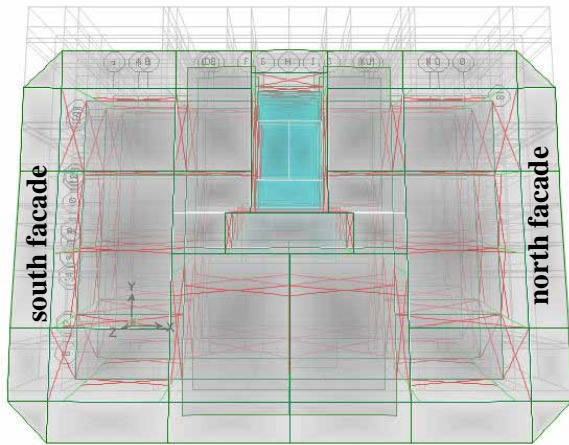


(a) South facade

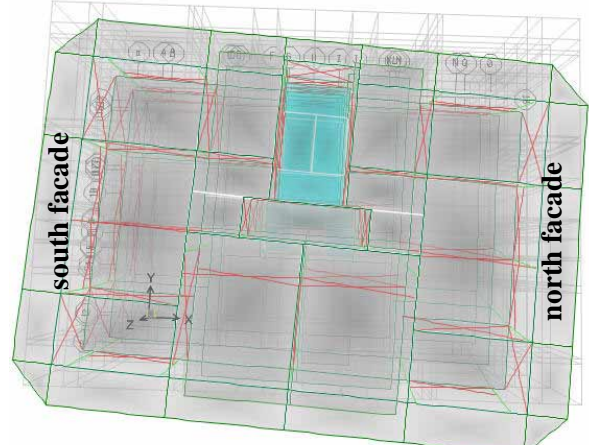


(b) North facade

Figure 30. Calculated damage progression (ETABS) at extensive damage state (HAZUS 99).



(a) at slight damage grade (HAZUS 99)



(b) at extensive damage grade (HAZUS 99)

Figure 31. First mode shape - transverse direction (DUZ-1).

none has failed. Thus the structure retains its regularity, and the first mode shape shows purely transversal displacements, as pictured in Figure 31 (a). When load levels are raised further, the first failure of an infill occurs in the north façade. The asymmetries causing the differences in the reaction of the northern and the southern side are very small at the beginning. The subsequent redistribution of loads, however, leads to a chain reaction, during which the walls on the northern side fail one after the other, until only those at the top level are left, as illustrated in Figure 30 (a). The southern side remains only slightly damaged, as shown in Figure 30 (b). This effect causes significant torsional motions in the 1st mode shape at extensive HAZUS 99 damage state (Figure 31 b).

DUEZCE 1 time history excitation

In an attempt to simulate the seismic impact caused by the Kocaeli earthquake in August 1999 on the building DUZ-1, the east-west component of the time history recorded at the meteorology station was scaled to $PGA=0.18g$ (cf. Figure 25). The resulting peak ground acceleration level arises from attenuation relationships that take into account the intensity observed at the building site. Following the procedure of the capacity spectrum method described in ATC-40, a reaction within the linear elastic range results for the estimated realistic seismic excitation (cf. Figure 26). Indeed no damage was observed on this particularly strong building after the earthquake.

More vulnerability calculations were performed with the same time history scaled to greater PGA levels. At a PGA of $0.36g$ slight damage can be observed in the model, while $PGA=0.54g$ and $PGA=0.72g$ cause moderate to extensive damage in the structure (Figure 26). While $PGA=0.36g$ meets the conditions of the mainshock measured at the meteorology station, the PGA level of $0.72g$ is a quite unrealistic value at the building site of DUZ-1. Consequently, the building is assessed as a good design which would probably not fail during an earthquake.

DUEZCE 1 design spectrum excitation

According to Turkish specifications, this structure requires a design spectrum corresponding to seismic zone Z4 ($PGA=0.4g$) and soft soil conditions. The function of the building as a health care center requires a high building importance factor of $I=1.5$, which results in high spectral design accelerations (Figure 27). In order to apply the N2-method proposed by Fajfar [3], a bilinear approximation according to the equal energy rule is derived from the capacity spectrum. The reduction factor $\mu=1.9$, which leads to the inelastic demand spectrum, is derived from four factors: the strength and deformation capacity of the system, the relation between building period T and the spectrum period T_C and, finally, the spectral acceleration of the design spectrum. According to the calculation with the N2 method, a moderate damage would occur given an earthquake corresponding to the design spectrum (cf. Figure 28).

CONCLUSIONS

An efficient approach to the problem of determining damage grades is seen in the identification of critical elements for typical building types, the state of which reflects the remaining capacity of the building [10].

An important aspect in the calculation of the capacity curves presented here is the parallel use of two engineering software applications with different fundamental theories: Classical beam versus finite element theory. In this case, both ways led to similar results. The implementation of an asymmetric non-linear material law to one of the applications was necessary.

The collection of structural data described in Part 1 [8] provided the basis for establishing realistic models. Calibrating the stiffness of the models by comparison to the dynamic recordings of the structure led to a reduction factor of approximately 0.5 for structures with slight damage. Interestingly, this

corresponds to the recommendation given in EC 8 for the stiffness of cracked concrete. With the exception of one case, structures with no visible damage required no stiffness reduction.

Calculations using time histories representing the impact of the 1999 Kocaeli earthquake showed moderate or no damage in the presented buildings, corresponding well with observations. Both sites were located at some distance from the epicenter (İzmit-2a: 15 km, Düzce-1: 110 km). It remains to be seen whether similar results can be achieved when buildings with more extensive damage are involved.

Estimations of structural performance were conducted using both scaled time histories and site-specific response spectra reflecting the particularities of instrumentally classified subsoil conditions (see part 1 of the paper: Lang et al. [8]). The results indicate that the vulnerability of the average Turkish multistoried residential buildings, of which İzmit-2a is an example, does not fulfill the requirements by the design code. Positive characteristics of this building group are the regularity and tight spacing of the column grid, as well as the large, wall-like dimensions of the columns. On the other hand, the most striking negative factor is the absence of increased shear reinforcement at connection points, which is a major contributor to the low ductility and typical early failure of the ground floor columns. Other problematic aspects are the large discrepancies in horizontal strength of the two main building axes and the erratic influence of the infills, which may lead to weak story or torsional effects. The building Düzce-1, which is of great importance, behaved favorably in the investigations and is regarded as sufficiently secure.

REFERENCES

1. Applied Technology Council: ATC 40, "Seismic Evaluation and Retrofit of Concrete Buildings", Volume 1, Report No. SSC 96-01, Applied Technology Council, California, USA, November 1996.
2. Bucher Ch et al. "SLang- The Structural Language." Version 5.0.4, Institute of Structural Mechanics, Bauhaus-University Weimar, Germany, December 2003.
3. Fajfar P. "A nonlinear analysis method for performance based seismic design." *Earthquake Spectra* 2000; 16(3): 573-592.
4. Fajfar P, Dolšek M, Žarnić R, Gostič S. "Development of numerical methodologies for infilled frames." Towards European integration in seismic design and upgrading of building structures, Euroquake-project, Final report, February 2001.
5. Federal Emergency Management Agency: FEMA 306, "Evaluation of earthquake damaged concrete and masonry wall buildings", basic procedures manual, Washington D.C., USA, 1998.
6. Federal Emergency Management Agency (FEMA). "HAZUS 99 - Earthquake Loss Estimation Methodology." Technical manual, Washington D.C., United States, 1999.
7. Grünthal G (ed.), Musson R, Schwarz J, Stucchi M. "European Macroseismic Scale 1998." *Cahiers du Centre Européen de Géodynamique et de Séismologie*; Volume 15, Luxembourg, 1998.
8. Lang DH, Ende C, Schwarz J. "Vulnerability of RC frame structures in Turkish earthquake regions (Part 1): Instrumental testing." *Proceedings of the 13th World Conference on Earthquake Engineering 2004*, Vancouver, Canada; Paper no. 216.
9. Schott C, Swain TM, Schwarz J. "Calibration of nonlinear force-deformation relationships for RC frame systems with or without masonry infills and application of the Pushover analysis: Case studies on the basis of multistory RC structures representative for Turkish earthquake regions." Unpublished technical report, Earthquake Damage Analysis Center, Bauhaus-University Weimar, Germany, November 2003.
10. Swain TM, Schwarz J. "Formulation of a Concept for Assignment of Damage Grades According to EMS-98 by Consideration of Associated Damage Patterns." Internal technical report, Earthquake Damage Analysis Center, Bauhaus-University Weimar, Germany, January 2004.